

Towards a theory of wall-bounded super-fluid turbulence

V. S. Lvov

in collaboration with

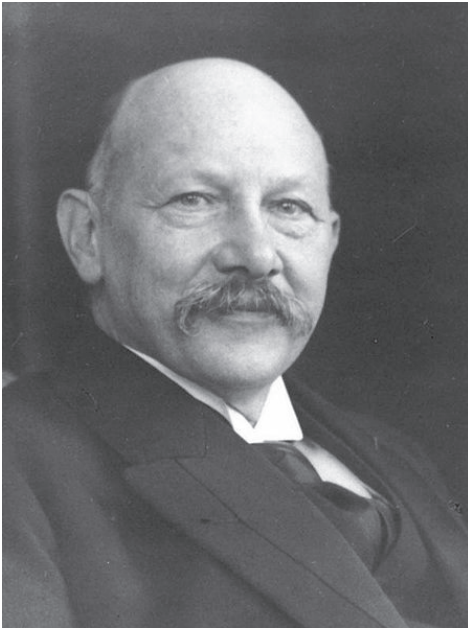
D. Khomenko, L. Kondaurova, P. Mishra, A. Pomyalov and I. Procaccia

OUTLINE

- Superfluids: experiments and theory
- Superfluid Dynamics and Turbulence
- Hall-Vinen-Bekarevich-Khalatnikov coarse-grained 2-fluid equations
- Closure problems in the Vinen equation and suggested resolution
- Starting from first principles: Analytical results
- Numerical simulations and comparison with analytical closures
- Summary of the results and perspectives

● *Superfluids: experiments and theory*

Heike Kamerlingh-Onnes

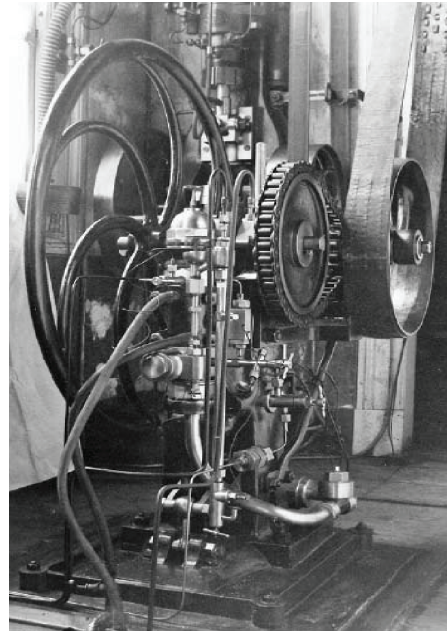


Nobel prize 1913

"for his investigations on the properties of matter at low temperatures which led, inter alia, to the production of liquid helium".

K-O discovered in 1911 **superconductivity**.

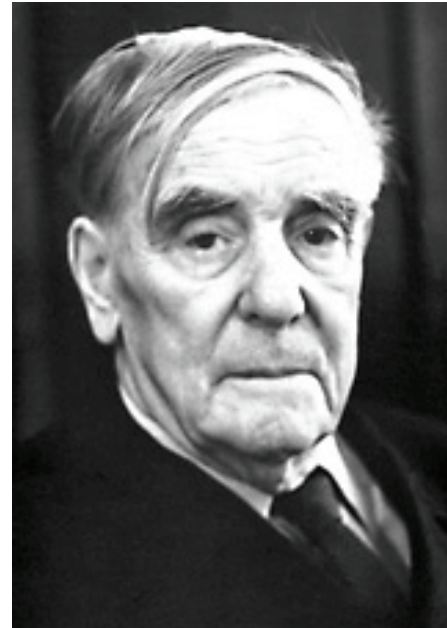
using this Compressor



liquefied He at $T = 4.2$ K in July 10, 1908.
K-O & coworkers in 1924 discovered density change at $T = 2.18$ K.

Keesom & Wolfke, 1928: this is a phase transition
 $\text{He I} \Leftrightarrow \text{He II}$.

Piotr Leonidovich Kapitza



Nobel prize 1978

"for his basic inventions and discoveries in the area of low-temperature physics". P.L. Kapitza in Moscow discovered and named in 1937 **superfluidity of ^4He**

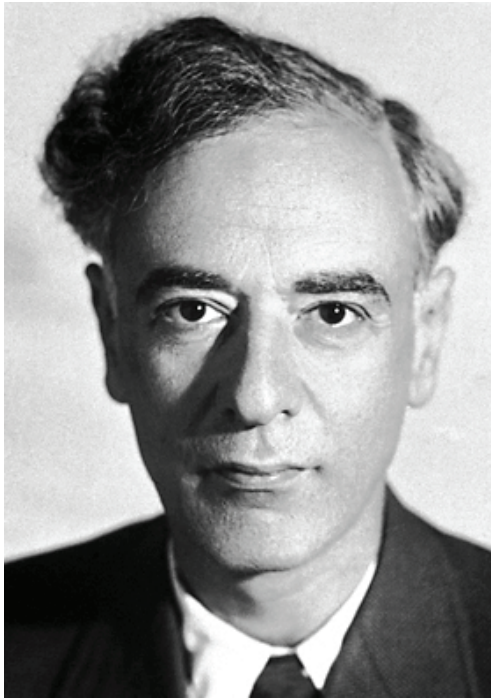
Jack Allen



and his student **Donald Missener**



independently discovered superfluidity in PLK's Cambridge lab.



Lev Davidovich Landau
Nobel Prize, 1962

"for his pioneering theories for condensed matter, especially liquid helium".
In particular, he quantized in 1941 the Tisza-1940 two-fluid model and suggested Andronikashvili's 1946 experiment on oscillating in He II discs.

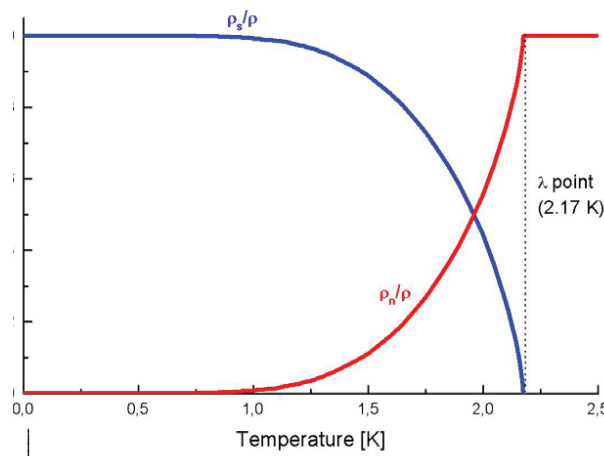
Elepter Luarsabovich
Andronikashvili



Laszlo
Tisza



Its period and damping measures densities of superfluid, ρ_s and normal, ρ_n , components:



Landau-Tisza two fluid model

for superfluid, \mathbf{V}_n , and normal \mathbf{V}_s velocities:

$$\rho_s \frac{D\mathbf{v}_s}{Dt} = -\frac{\rho_s}{\rho} \nabla p + \rho_s S \nabla T - \mathbf{F}_{ns}$$

$$\rho_n \frac{D\mathbf{v}_n}{Dt} = -\frac{\rho_n}{\rho} \nabla p - \rho_s S \nabla T + \eta \nabla^2 \mathbf{v}_n + \mathbf{F}_{ns}$$

predicts "second sound", critical velocity, etc.
Here: S – entropy, T – temperature and \mathbf{F}_{ns} is the mutual friction force

Quantum mechanical description of He II

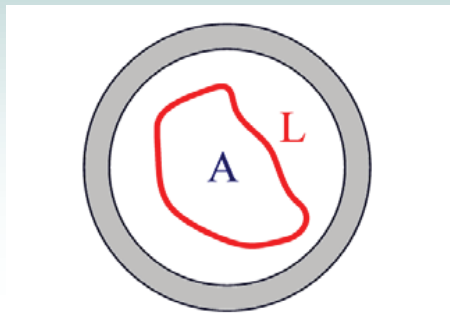
Macroscopic wave function

$$\Psi = \sqrt{\rho_s} \exp\{i\varphi(r,t)\}$$

$$\hat{p} = i\hbar\nabla \longrightarrow \mathbf{v}_s = \frac{\hbar}{m_4} \nabla\varphi \longrightarrow \text{curl}\mathbf{v}_s = 0$$

Circulation –singly connected region

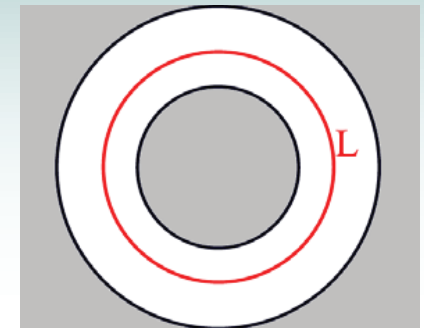
$$\Gamma = \oint_L \mathbf{v}_s \cdot d\mathbf{l} = 0$$



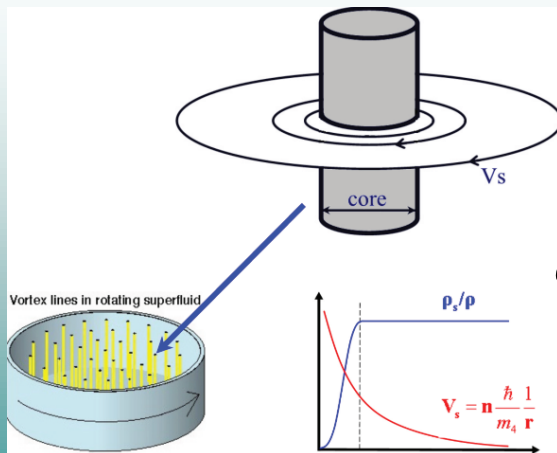
Circulation- multiply connected region

$$\Gamma = \oint_L \mathbf{v}_s \cdot d\mathbf{l} = n \frac{h}{m_4} = n\kappa$$

$$\kappa \cong 10^{-7} \text{ m}^2 / \text{s}$$



Quantized vortices in He II

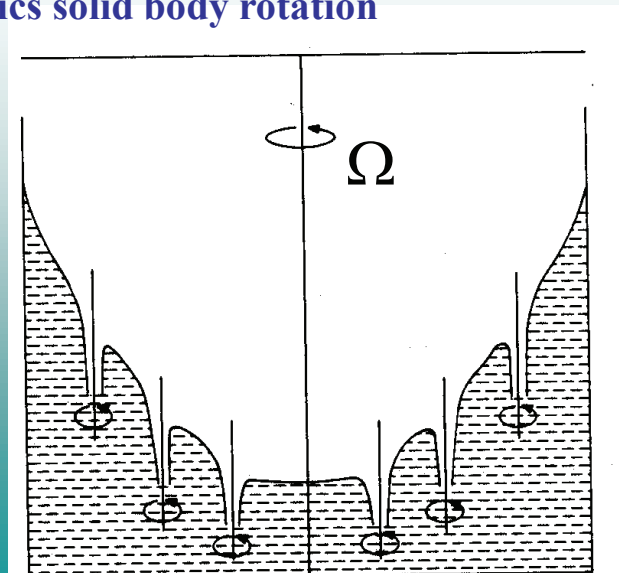


vorticity

$$\omega_N = 2\Omega \cong \langle \omega_S \rangle \cong \kappa L$$

Rotating bucket of He II

-thanks to the existence of rectilinear vortex lines
He II mimics solid body rotation



• *Superfluid Dynamics and Turbulence*

Turbulence in a superfluid was predicted first by **Richard Feynman** in **1955** and found experimentally (in counterflow ^4He) by **Henry Hall** and **Joe Vinen** in **1956**.

1.3.1 Normal fluid vs. superfluid at $T \rightarrow 0$ limit:

- Normal fluid kinematic viscosity $\nu \neq 0$ vs. $\nu \equiv 0$ in superfluids;
- Two scales in normal fluids: Outer scale L and dissipative micro-scale $\eta \ll L$;
- Two additional scales in superfluids due to quantization of vortex lines:

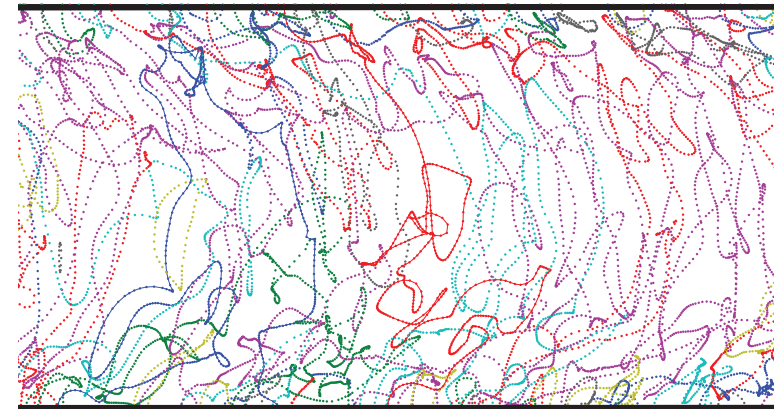
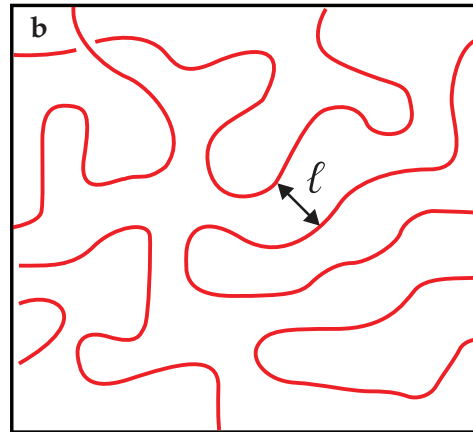
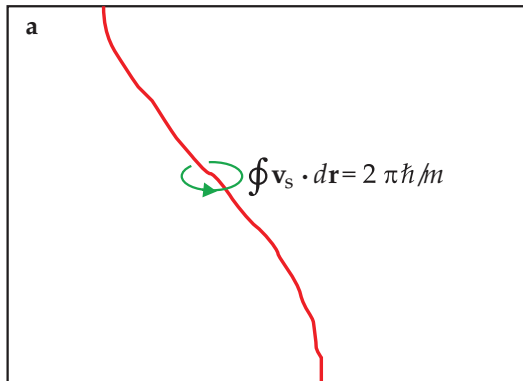
↓ vortex core diameter a_0 ↓

↓ inter-vortex distance ℓ ↓

↓

Outer scale \mathcal{L}

↓



In ^4He $a_0 \simeq 1 \text{ \AA}$, in ^3He $a_0 \simeq 800 \text{ \AA}$. Experimentally, in both ^4He and ^3He , $\Lambda \equiv \ln\left(\frac{\ell}{a_0}\right) \simeq 12 \div 15$.

- *Hall-Vinen-Bekarevich-Khalatnikov coarse-grained two-fluid equations*

In hydrodynamic region of scales $R \gg \ell$ one can neglect the quantization of vortex lines and make use of the coarse-grained two fluid equation for velocities of the superfluid and normal components \mathbf{u}_s and \mathbf{u}_n , with densities ρ_s and ρ_n and pressures p_s and p_n

$$\rho_s \left[\frac{\partial \mathbf{u}_s}{\partial t} + (\mathbf{u}_s \nabla) \mathbf{u}_s \right] - \nabla p_s = -\mathbf{F}_{ns}, \quad p_s = \frac{\rho_s}{\rho} [p - \rho_n |\mathbf{u}_s - \mathbf{u}_n|^2], \quad (1a)$$

$$\rho_n \left[\frac{\partial \mathbf{u}_n}{\partial t} + (\mathbf{u}_n \nabla) \mathbf{u}_n \right] - \nabla p_n = \rho_n \nu \Delta \mathbf{u}_n + \mathbf{F}_{ns}, \quad p_n = \frac{\rho_n}{\rho} [p + \rho_s |\mathbf{u}_s - \mathbf{u}_n|^2], \quad (1b)$$

coupled by the **the mutual friction** between superfluid and normal components of the liquid mediated by quantized vortices which transfer momenta from the superfluid to the normal subsystem and vice versa:

$$\mathbf{F}_{ns} = -\rho_s \{ \alpha' (\mathbf{u}_s - \mathbf{u}_n) \times \boldsymbol{\omega}_s + \alpha \hat{\boldsymbol{\omega}}_s \times [\boldsymbol{\omega}_s \times (\mathbf{u}_s - \mathbf{u}_n)] \} \approx \alpha \rho_s \omega_T (\mathbf{u}_s - \mathbf{u}_n), \quad \omega_T = \kappa \mathcal{L} \quad (1c)$$

Here we used for \mathbf{F}_{ns} a simple closure (approximation) [Ref.]¹ written in terms of the vortex-line density $\mathcal{L}(\mathbf{r}, t)$. Eqs (1) are very similar to the Navier-Stokes equation. Therefore in a theory of large-scale superfluid turbulence, including wall-bounded (i.e. channel turbulent flow), we can use numerous tools, developed in the theory of classical HD turbulence. The only essential difference is the mutual friction, controlled by the vortex-line density \mathcal{L} , dominated by small scales. Thus the classical models of channel flows (involving only characteristics of large-scale eddies – mean velocity and Reynolds stress $\langle \delta v_i \delta v_j \rangle$ profiles), should be accompanied by equation $\mathcal{L}(\mathbf{r}, t)$.

An additional equation for the vortex-line density $\mathcal{L}(\mathbf{r}, t)$ the subject of my talk.

¹ V. S. L'vov, S. V. Nazarenko and G. E. Volovik, JETP Letters, v. 80, 535-539 (2004)

- *Closure problems in the Vinen equation and suggested resolution:*

Consider Vinen-1957 phenomenological equation for $\mathcal{L}(t)$ for homogeneous counterflows:

$$\frac{d\mathcal{L}(t)}{dt} = \mathcal{P}(t) - \mathcal{D}(t) . \quad (2a)$$

Production term $\mathcal{P}(t) \propto \alpha$ – the growth of \mathcal{L} due to the extension of the vortex rings by **mutual friction**, which is caused by the difference between the velocities of the normal and super components (“the counterflow velocity” V_{ns} .)

Decay term, $\mathcal{D}(t) \propto \alpha$ is again caused by the mutual friction due to fast moving normal fluid components and is independent of V_{ns} .

Dimensional reasoning:

$$\mathcal{P} \Rightarrow \mathcal{P}_{\text{cl}} = \alpha \kappa \mathcal{L}^2 F(x) , \quad \mathcal{D} \Rightarrow \mathcal{D}_{\text{cl}} = \alpha \kappa \mathcal{L}^2 G(x) , \quad x = V_{\text{ns}}^2 / \kappa^2 \mathcal{L} . \quad (2b)$$

Here $F(x)$ and $G(x)$ are dimensionless functions of the dimensionless argument x .

Earlier suggestions:

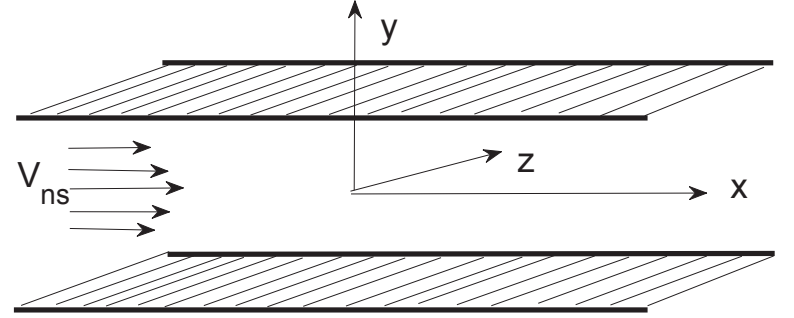
$$\mathcal{P}_{\text{cl}} \Rightarrow \mathcal{P}_1 = \alpha C_1 \mathcal{L}^{3/2} |V_{\text{ns}}| , \quad \text{or} \quad \mathcal{P}_{\text{cl}} \Rightarrow \mathcal{P}_2 = \alpha C_2 \mathcal{L} V_{\text{ns}}^2 / \kappa . \quad (3a)$$

$$\mathcal{D}_{\text{cl}} = \alpha C_{\text{dec}} \kappa \mathcal{L}^2 \quad \text{assuming that } \mathcal{D}_{\text{cl}} \text{ is independent of } V_{\text{ns}} . \quad (3b)$$

Neither Vinen’s nor later experimental attempts succeeded to distinguish between \mathcal{P}_1 and \mathcal{P}_2 .

To resolve the closure uncertainty

we suggest to study the channel flow in which $\mathcal{P}_{\text{cl}}(\mathbf{y})$ and $\mathcal{D}_{\text{cl}}(\mathbf{y})$ have nontrivial profiles. For that goal we suggest inhomogeneous equation of motion for the field $\mathcal{L}(\mathbf{r}, t)$, which in the channel geometry \Rightarrow has the form \Downarrow



$$\frac{\partial \mathcal{L}(\mathbf{y}, t)}{\partial t} + \frac{\partial}{\partial \mathbf{y}} \mathcal{J}_{\text{cl}}(\mathbf{y}, t) = \mathcal{P}_3(\mathbf{y}, t) - \mathcal{D}_{\text{cl}}(\mathbf{y}, t) . \quad (4a)$$

Here we have added a vortex-line density flux $\mathcal{J}(\mathbf{r}, t)$, which we suggest to model as follows:

$$\mathcal{J}_{\text{cl}}(\mathbf{r}, t) = -C_{\text{flux}} (\alpha/2\kappa) \nabla V_{\text{ns}}^2 . \quad (4b)$$

We will show that none of the closures for the production term \mathcal{P}_1 and \mathcal{P}_2 , given by Eqs.(3) are correct. We propose yet a third form of \mathcal{P} [corresponding to $f(x) \propto x^{3/2}$]:

$$\mathcal{P}_{\text{cl}} \Rightarrow \mathcal{P}_3 = \alpha C_{\text{prod}} \sqrt{\mathcal{L}} V_{\text{ns}}^3 / \kappa^2 , \quad (4c)$$

which fits the data that are presented below significantly better than either of the equations (3).

We show that Eqs. (4) may serve as a basis for future studies of wall-bounded superfluid turbulence.

- *Starting from first principles: Analytical results*

Using Biot-Savart equation for the quantized vortex lines supplemented by the mutual friction, Schwarz derived the equation of motion for the length of the vortex-line segment $\delta\xi$:

$$\frac{1}{\delta\xi} \frac{d\delta\xi}{dt} \approx \alpha \mathbf{V}_{\text{ns}}(\mathbf{s}, t) \cdot (\mathbf{s}' \times \mathbf{s}''). \quad (5a)$$

Here $\mathbf{s}(\xi, t)$ is the coordinate of the quantized vortex lines parameterized by the arc-length ξ ; $\mathbf{s}' = d\mathbf{s}/d\xi$, $\mathbf{s}'' = d^2\mathbf{s}/d\xi^2$. The counterflow velocity \mathbf{V}_{ns} is

$$\mathbf{V}_{\text{ns}} = \mathbf{V}^{\text{n}} - \mathbf{V}^{\text{s}}, \quad \mathbf{V}^{\text{s}} = \mathbf{V}_0^{\text{s}} + \mathbf{V}_{\text{BS}}. \quad (5b)$$

The super-fluid velocity \mathbf{V}^{s} includes the macroscopic potential part \mathbf{V}_0^{s} , and the Biot-Savart velocity \mathbf{V}_{BS} , defined by the entire vortex tangle configuration \mathcal{C}

$$\mathbf{V}_{\text{BS}} = \frac{\kappa}{4\pi} \int_{\mathcal{C}} \frac{(\mathbf{s} - \mathbf{s}_1) \times d\mathbf{s}_1}{|\mathbf{s} - \mathbf{s}_1|^3} = \mathbf{V}_{\text{LIA}}^{\text{s}} + \mathbf{V}_{\text{nl}}^{\text{s}}. \quad (5c)$$

The logarithmically divergent (when $\mathbf{s}_1 \rightarrow \mathbf{s}$) integral (5c) can be regularized by using the vortex core radius a_0 and the mean vortex line curvature radius $R = 1/\tilde{S}$.

The main contribution to \mathbf{V}_{BS} , known as the ‘‘Local Induction Approximation’’ (LIA), originates from integrating over scales between a_0 and R , i.e. $a_0 \leq |\mathbf{s}_1 - \mathbf{s}| \leq R$:

$$\mathbf{V}_{\text{LIA}}^{\text{s}} = \beta \mathbf{s}' \times \mathbf{s}'', \quad \beta \equiv (\kappa/4\pi) \ln(R/a_0). \quad (5d)$$

The non-local term $\mathbf{V}_{\text{nl}}^{\text{s}}$ is produced by the rest of the vortex configuration, \mathcal{C}' , with $|\mathbf{s}_1 - \mathbf{s}| > R$:

$$\mathbf{V}_{\text{nl}}^{\text{s}} = \frac{\kappa}{4\pi} \int_{\mathcal{C}'} \frac{(\mathbf{s} - \mathbf{s}_1) \times d\mathbf{s}_1}{|\mathbf{s} - \mathbf{s}_1|^3}. \quad (5e)$$

Integrating Eq. (5a),

$$\frac{1}{\delta\xi} \frac{d\delta\xi}{dt} \approx \alpha \mathbf{V}_{\text{ns}}(\mathbf{s}, t) \cdot (\mathbf{s}' \times \mathbf{s}''), \quad (5a)$$

over the vortex tangle in a fixed volume Ω residing in slices between y and $y + \delta y$, going over all x and z one gets Eq. (4a),

$$\frac{\partial \mathcal{L}(y, t)}{\partial t} + \frac{\partial}{\partial y} \mathcal{J}(y, t) = \mathcal{P}(y, t) - \mathcal{D}(y, t), \quad (4a)$$

for $\mathcal{L}(y, t) \equiv \int_{\mathcal{C}_\Omega} d\xi / \Omega$ with the following identification for the

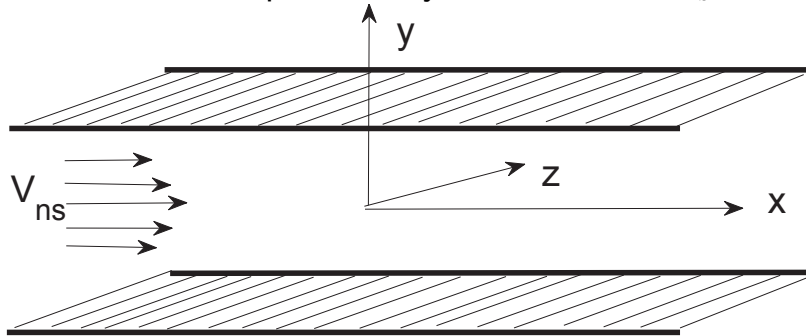
$$\text{Production term: } \mathcal{P}(y, t) = \frac{\alpha}{\Omega} \int_{\mathcal{C}_\Omega} d\xi (V^n - V_0^s - V_{\text{nl}}^s) \cdot (\mathbf{s}' \times \mathbf{s}''), \quad (6a)$$

$$\text{Decay term: } \mathcal{D}(y, t) = \frac{\alpha\beta}{\Omega} \int_{\mathcal{C}_\Omega} d\xi |s''|^2 = \alpha\beta \mathcal{L} \tilde{S}^2, \quad \text{and} \quad (6b)$$

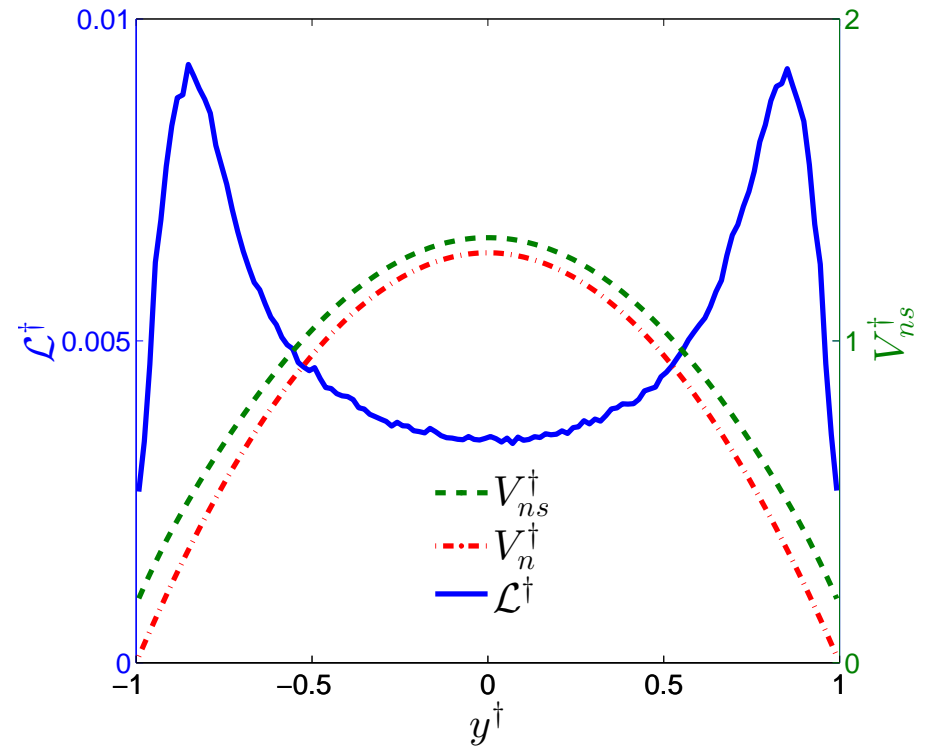
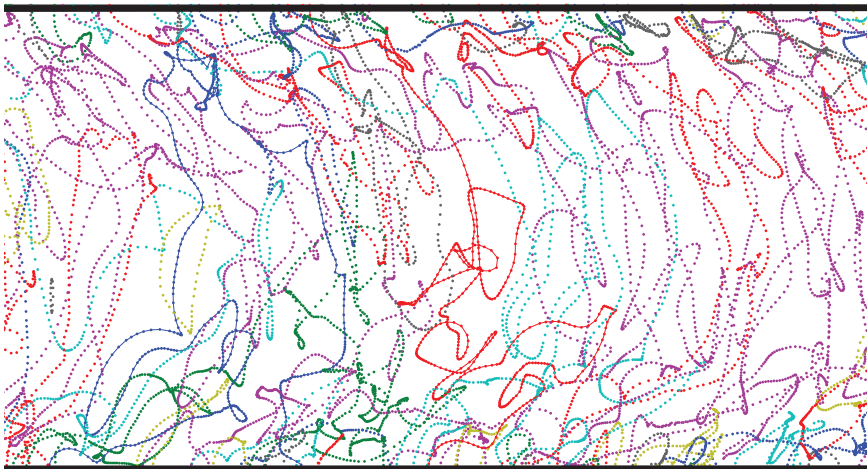
$$\text{Flux term: } \mathcal{J}(y, t) = \frac{\alpha}{\Omega} \int_{\mathcal{C}_\Omega} d\xi V_{\text{ns},x} s'_z. \quad (6c)$$

• *Numerical simulations and comparison with analytical closures*

where carried out in the channel geometry in the framework of the vortex filament method (Biot-Savart equations for the quantized vortex lines, supplemented by the mutual friction force). Temperature $T = 1.6$ K, $V_n(0) = 1$ cm/s, $h = 0.5$ mm, full slip boundary conditions for V_s .



Example of the resulting vortex line configuration:



Prescribed normal velocity profile –

red dash-dotted line

Resulting normalized counterflow velocity profile

$V_{ns}^\dagger(y)$ – green dash line — — ,

Vortex line density profile $\mathcal{L}^\dagger(y)$, blue solid line.

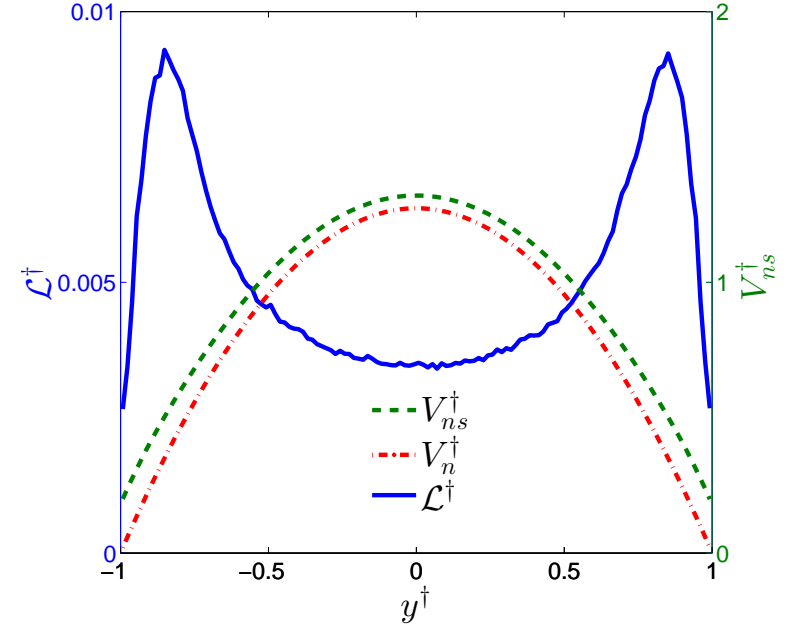
$$y^\dagger = y/h, \quad V^\dagger = V/\sqrt{\langle V_{ns}^2 \rangle}, \quad \mathcal{L}^\dagger = \kappa^2 \mathcal{L} / \langle V_{ns}^2 \rangle .$$

– Comparison of the numerics to the analytical closure forms –Parabolic profile

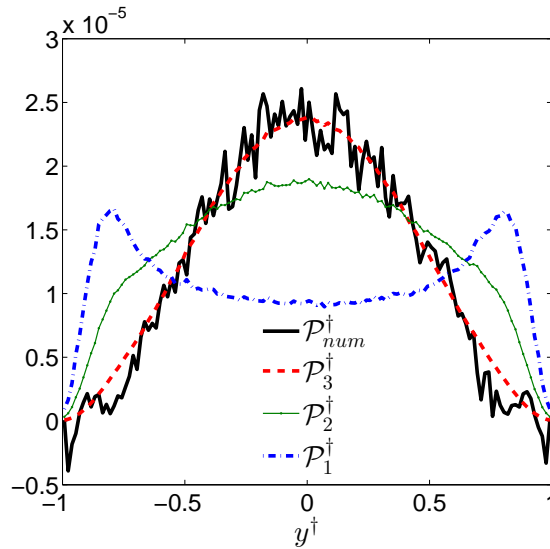
Panel a: Comparison of the numerical data (black lines) to the competing production forms of the Vinen equation: blue line $-\mathcal{P}_1$, green line $-\mathcal{P}_2$, and red line – our suggestion \mathcal{P}_3 .

Panel b: Comparison of the numerical data for decay with the traditional analytical closure Eq.(3b),

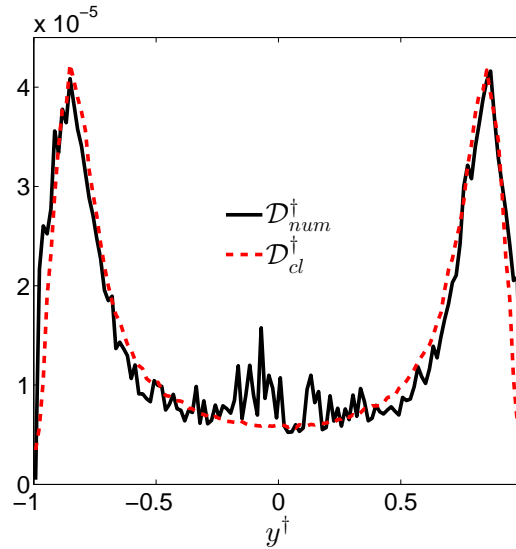
Panel c: Comparison of the numerical data for the flux term J with suggested closure Eq.(4b)



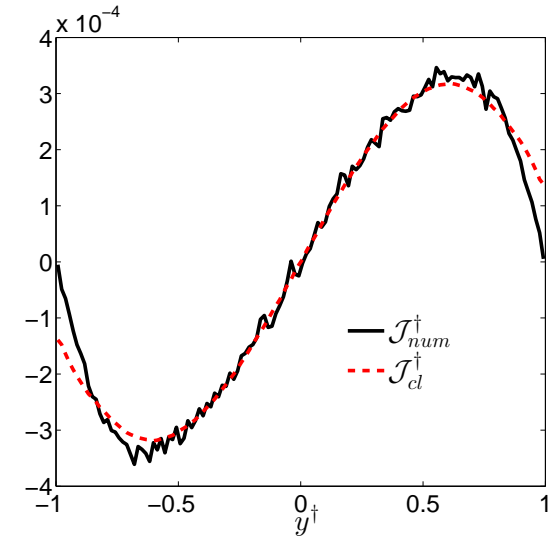
a: production



b: decay



c: flux

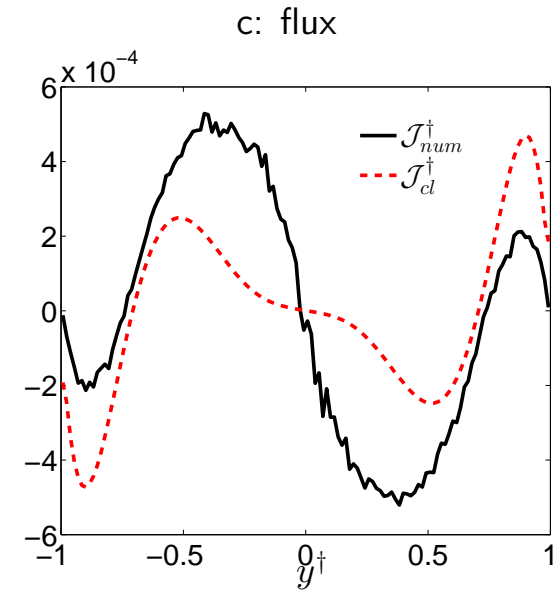
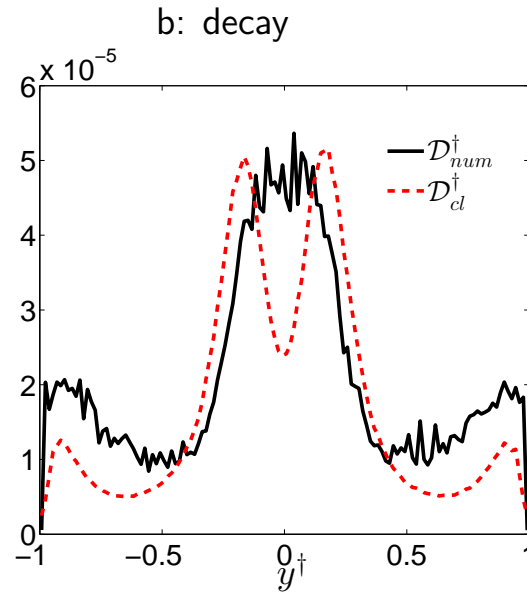
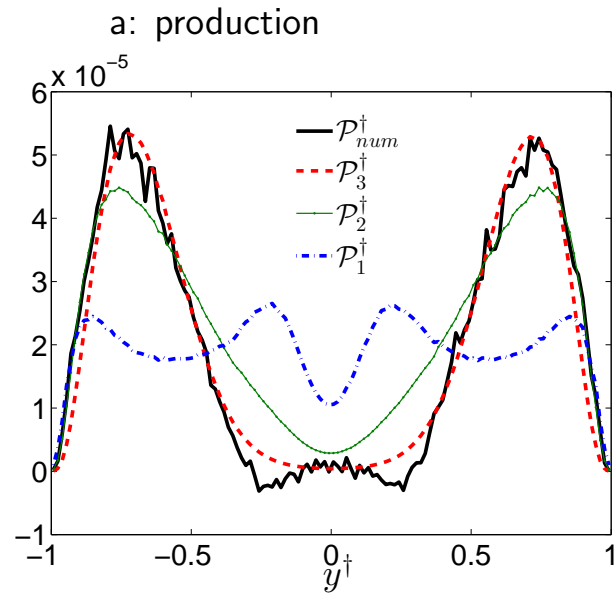
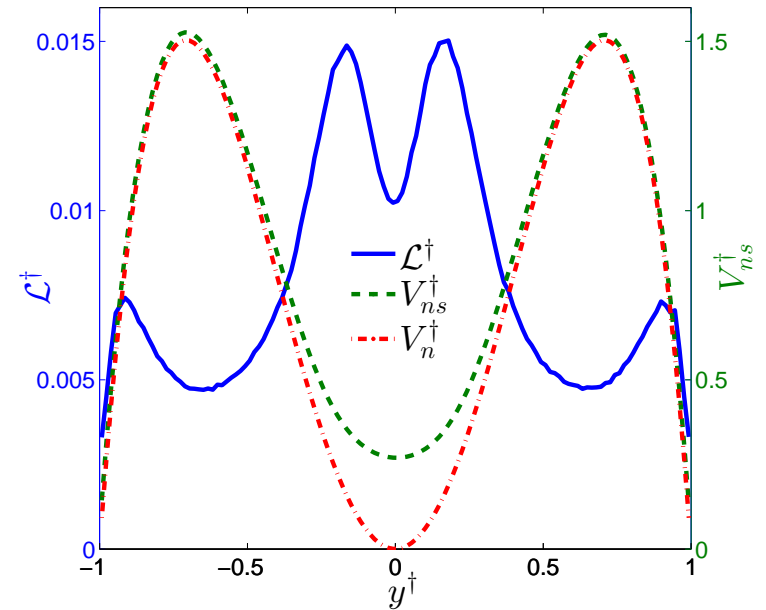


- Comparison of the numerics to the analytical closures –Non-parabolic profile

Panel a: Comparison of the numerical data (black lines) to the competing production forms of the Vinen equation: blue line $-\mathcal{P}_1$, green line $-\mathcal{P}_2$, and red line – our suggestion \mathcal{P}_3 .

Panel b: Comparison of the numerical data for decay with the traditional analytical closure Eq.(3b),

Panel c: Comparison of the numerical data for the flux term J with suggested closure Eq.(4b)



- *Summary and perspectives*

– We consider inhomogeneous equation for the vortex line density

$$\frac{\partial \mathcal{L}}{\alpha \partial t} - \frac{C_{\text{flux}}}{2\kappa} \frac{\partial^2 V_{\text{ns}}^2}{\partial y^2} = \frac{C_{\text{prod}}}{\kappa^2} \sqrt{\mathcal{L}} V_{\text{ns}}^3 - C_{\text{dec}} \kappa \mathcal{L}^2 .$$

– The suggested closure for the **production term** using the counterflow velocity and the vortex line density profiles can be considered as highly promising.

– However, the **traditional closure for the decay term** and **suggested closure for the flux term** are sensitive to the counterflow velocity profile and work well for monotonic profiles, close to the parabolic ones. In general case they require additional tangle characteristics.

– The first candidate is the tangle curvature; the tangle anisotropy also can be important.

– Much more work in this direction is required to develop a consistent theory of the wall-bounded superfluid turbulence.